

Sevoflurane Inhibits the Progression of Gallbladder Cancer Through Activating Endoplasmic Reticulum Stress and Reducing Glycolysis by Downregulating ROCK1

Yuwen Lao¹, Dong Zhao¹, Lei Zhang¹, Shuangjiang Li^{2,*}, Huayan Lv^{1,*}

¹Department of Anesthesiology, Affiliated Jinhua Hospital, Zhejiang University School of Medicine, 321000 Jinhua, Zhejiang, China

²Department of Anesthesiology, The Second Affiliated Hospital, Zhejiang University School of Medicine, 310000 Hangzhou, Zhejiang, China

*Correspondence: 2517096@zju.edu.cn (Shuangjiang Li); lvhuayan2009@163.com (Huayan Lv)

Submitted: 7 November 2025 Revised: 20 November 2025 Accepted: 5 January 2026 Published: 20 February 2026

Background: Gallbladder cancer (GBC) is a highly aggressive malignancy with a notoriously poor prognosis and limited treatment options. Intriguingly, beyond its established perioperative applications, the inhalational anesthetic Sevoflurane has garnered attention for its potential anti-tumor effects, demonstrating the ability to inhibit progression in various cancers. However, its specific impact and the underlying molecular mechanisms in GBC remain largely unexplored. This study systematically investigated the anti-cancer property of Sevoflurane in GBC and associated signaling pathways.

Methods: Sevoflurane at 1.7%, 3.4% and 5.1% concentrations was separately employed to treat human intestinal biliary epithelial cells (HIBEpic) and GBC-SD cells. GBC-SD cells were also pretreated with an endoplasmic reticulum (ER) stress inhibitor Salubrinal, or transfected with Rho-associated coiled-coil containing protein kinase 1 (ROCK1)-overexpressing vectors/short hairpin RNA against ROCK1. Cell viability, migration and invasion, colony formation, and apoptosis were determined using Cell Counting Kit-8, Transwell, colony formation, and flow cytometry assays, respectively. Special kits were used to detect levels of glucose uptake, lactate and adenosine triphosphate (ATP) in GBC-SD cells. ROCK1 expression and levels of ROCK1, activating transcription factor 4 (ATF4) and C/EBP-homologous protein 10 (CHOP) were quantified by quantitative real-time reverse transcription polymerase chain reaction and Western blot analyses, respectively.

Results: Sevoflurane exposure inhibited malignant phenotypes, promoted apoptosis and expressions of ATF4 and CHOP, and reduced ROCK1 expression and levels of glucose uptake, lactate and ATP in GBC-SD cells, while Salubrinal pretreatment reversed the upregulated trends of ATF4 and CHOP ($p < 0.05$). ROCK1 was highly expressed in different GBC cell lines ($p < 0.05$). ROCK1 overexpression enhanced malignant phenotypes, promoted levels of glucose uptake, lactate and ATP, and suppressed apoptosis in GBC-SD cells, while ROCK1 silencing reversed these alterations ($p < 0.05$). Meanwhile, ROCK1 overexpression reversed the effects of Sevoflurane on GBC-SD cells ($p < 0.05$).

Conclusion: Sevoflurane suppresses GBC progression by activating ER stress and reducing glycolysis via ROCK1 downregulation.

Keywords: Sevoflurane; gallbladder cancer; endoplasmic reticulum stress; glycolysis; Rho associated coiled-coil containing protein kinase 1

Introduction

Gallbladder cancer (GBC) is a comparatively rare malignant tumor characterized by a mass in the gallbladder (GB) and the GB cavity, as well as focal or diffuse thickening of the GB wall [1]. Despite countless studies on GBC, surgical excision remains the primary therapy [2]. Due to its highly invasive nature and insidious onset, only 20% of patients are eligible for surgical excision at the time of diagnosis, while ineligible patients have particularly terrible prognoses, with the total mortality rate rising each year [3]. Thereby, the development of efficient medicines represents one of the most urgent priorities in GBC management.

Sevoflurane is a colorless, volatile, non-flammable liquid with a special odor and a halogenated inhalational anesthetic widely used in inpatient and outpatient surgery in both adults and children [4]. Besides, it also physiologically and pathologically mediates cellular activities such as cell apoptosis and differentiation [5–7], ferroptosis [8], and inflammation [9]. Notably, the role of Sevoflurane in alleviating the malignant biological behavior has been demonstrated in lung [10], breast [11], and cervical cancers [12]. Nevertheless, whether Sevoflurane exerts similar effects in GBC and the underlying mechanisms remain obscure.

Rho-associated coiled-coil containing protein kinase 1 (ROCK1) encodes a serine/threonine kinase that is acti-

vated upon binding to the GTP-bound form of Rho [13]. The RhoA/ROCK1 pathway is one of most important pathways in tumor cell motility and morphogenesis, which is associated with cell metastasis [14,15]. Incidentally, glycolysis is known as the process of turning glucose into pyruvate and lactate, accompanied by adenosine triphosphate (ATP) production [16]. Reportedly, ROCK1 may have the ability to mediate glycolysis in pancreatic cancer [17]. Altogether, ROCK1 takes part in the glycolysis of tumor cells and the progression of cancers.

As is known to all, the endoplasmic reticulum (ER) is an organelle related to protein aggregation, processing, folding, and modification. Disruption of ER homeostasis triggers ER stress as a compensatory mechanism to restore equilibrium, primarily through activation of the unfolded protein response and ER overload response. However, when an imbalance exists persistently in ER, ER stress even induces apoptotic pathways to eliminate abnormal cells [18,19]. Besides, ER stress impacts cisimarin-induced GBC cell apoptosis [20]. Activating transcription factor 4 (ATF4)/C/EBP-homologous protein 10 (CHOP) mediates ER stress-induced pro-apoptosis signaling, thereby suppressing cancer progression [21].

Given the unknown influence of Sevoflurane in GBC and the undefined molecular mechanisms, we, based on existing findings, speculated that the anti-GBC activity of Sevoflurane may be related to its induction of endoplasmic reticulum stress and regulation of ROCK-mediated glycolysis. Herein, we explored whether Sevoflurane inhibits GBC cancer progression and the underlying mechanisms through a series of *in-vitro* experiments. As a result, ER stress and ROCK-mediated glycolysis were proven to play key roles in the anti-GBC effects of Sevoflurane. This study establishes the first complete signaling pathway from Sevoflurane to ER stress and then to ROCK-glycolysis axis, ultimately inhibiting the progression of GBC.

Materials and Methods

Cell Culture and Transfection

Human intestinal biliary epithelial cells (HIBEpic, 5100) were obtained from ScienCell Research Laboratories (Santiago, CA, USA). GBC cell lines GBC-SD (TCHu 16, National Collection of Authenticated Cell Cultures, Shanghai, China), as well as Mz-ChA-1 (CL0226) and QBC939 (CL0448, Fenghui Biotechnology Co., Ltd., Changsha, China) were purchased. They were immersed in Dulbecco's modified eagle medium (DMEM)/F12 medium (D0697, Sigma Aldrich, St. Louis, MO, USA) supplemented with 10% fetal bovine serum (FBS, 12106C, Sigma Aldrich, St. Louis, MO, USA), 100 µg/mL streptomycin (85886, Sigma Aldrich, St. Louis, MO, USA), and 100 U/mL penicillin (V900929, Sigma Aldrich, St. Louis, MO, USA) in a 37 °C incubator (5% CO₂). All cell lines were validated by STR profiling and confirmed to be mycoplasma-free.

Prior to transfection, ROCK1 full sequence was assembled into pcDNA3.1 vectors (VT1001, YouBio, Changsha, China) for constructing overexpressing vectors, with an empty vector as a negative control (NC, 5'-CTAGAGAACCCACTGCTTAC-3'). The short hairpin RNA against ROCK1 (ShROCK1, sense: 5'-GGTTGTTTCAGATTGAGAAA-3'; antisense, 5'-TTTCTCAATCTGAACAACC-3') and its NC Super-Silevcing ShRNA (ShNC, C03002) were all provided by GenePharma Co., Ltd. (Shanghai, China). The CDS region of ROCK1 can be found in the **Supplementary Material**.

As the confluence of cells in 96-well plates reached 70–90%, Lipofectamine 3000 Reagent (L3000001, ThermoFisher, Waltham, MA, USA) was used for transfection. Firstly, Lipofectamine 3000 Reagent and vectors/ShRNAs were diluted in Opti-MEM™ (31985062, ThermoFisher, Waltham, MA, USA). Vectors/ShRNAs were further mixed with 0.2 µL P3000 Reagent and incubated in diluted Lipofectamine 3000 Reagent (room temperature (RT), 10 min), which were later co-incubated with cells (37 °C, 48 h). Finally, quantitative real-time reverse transcription polymerase chain reaction (qRT-PCR) was performed to determine transfection efficiency.

Cell Treatment

After an ER stress inhibitor Salubrinal (324895, Sigma Aldrich, St. Louis, MO, USA) dissolved in dimethyl sulfoxide (D1435, Sigma Aldrich, St. Louis, MO, USA) was diluted in the medium to 20 µM, cells were cultured for 1 h [22].

HIBEpic and GBC-SD cells were treated with Sevoflurane at 1.7%, 3.4%, and 5.1% concentrations [23]. Concretely, cells in the plates were kept in an airtight glass chamber with inlet and outlet connectors. The inlet port was connected to an anesthesia machine (Cicero EM 8060; Dräger, Lübeck, Germany) with a Sevoflurane vaporizer (Kent Scientific Corporation, Torrington, CT, USA) for delivering Sevoflurane into the chamber. Following 6-h exposure, cells were transferred to a CO₂ incubator (37 °C) for an additional 24-h incubation.

Cell Viability Measurement

HIBEpic and GBC-SD cells (5 × 10³ cells/well) were grown in 96-well plates (48 h), and then incubated with 10 µL/well Cell Counting Kit-8 reagent (ab228554, Abcam, Cambridge, UK) (4 h, darkness). The absorbance of wells at 460 nm was measured using an enzyme-linked immunosorbent assay (ELISA) reader (Bio-Rad 680, Bio-Rad Laboratories, Inc., Hercules, CA, USA). Cell viability was determined as follows:

$$\text{Relative Cell viability (\%)} = \frac{(\text{Optical density (OD)}_{\text{Experimental}} - \text{OD}_{\text{blank}})}{(\text{OD}_{\text{Control}} - \text{OD}_{\text{blank}})} \times 100\%.$$

Colony Formation Assay

200 μL cells (1×10^3 cells/well) were cultured in 6-well plates for two weeks. When the colony formed, the medium was discarded. Cells were fixed with 4% paraformaldehyde (P1110, Solarbio, Beijing, China) (15 min, RT) and then colored with Giemsa (G1010, Solarbio, Beijing, China) (15 min, RT). After washing with phosphate-buffered solution (PBS, P1020, Solarbio, Beijing, China), cells were observed using a BX53F microscope (OLYMPUS, Tokyo, Japan), and cell colonies were quantified. Colony formation rate = (the number of cell colonies (≥ 50 per colony)/seeded cells) $\times 100\%$. Relative colony formation rate (%) = (Number of colonies in treatment group / Number of colonies in control group) $\times 100\%$.

Cell Migration and Invasion Assays

For the invasion and migration assays, Transwell chambers with 8- μm pore polycarbonate membranes (140644, ThermoFisher, Waltham, MA, USA) were pre-coated with or without Matrigel (E1270, Sigma Aldrich, St. Louis, MO, USA), respectively. Cells (1×10^4 cells/well in 100 μL serum-free medium) were seeded into the upper chamber of 24-well Transwell plates, while the lower chambers were filled with 600 μL of medium containing FBS. Then cells were cultured for 48 h before analysis. Only cells in the lower chamber underwent fixation (4% paraformaldehyde; 30 min) and staining (Giemsa; 30 min, RT). Invasion and migration were observed under a BX53F microscope ($\times 250$ magnification) and analyzed using the ColonyArea plugin of ImageJ (v. 5.0, Bio-Rad Laboratories, Inc., Hercules, CA, USA). Relative migration/invasion rate (%) was quantified and normalized to the control group as follows: (Mean GBC cell count in treatment group / Mean GBC cell count in control group) $\times 100\%$.

Glucose Uptake, Lactate and ATP Assays

Glucose/Glucose Oxidase Assay Kit (MP 22189, Invitrogen, Carlsbad, CA, USA), ATP Assay Kit (S0026, Beyotime, Shanghai, China), and Lactate Assay Kit (ab65330, Abcam, Cambridge, UK) were obtained from Biovision (Milpitas, CA, USA) and used in this part. Briefly, for glucose uptake determination, 1×10^6 cells were incubated with 100 μL Krebs-Ringer-Phosphate-HEPES buffer containing 2% Bovine Serum Albumin (A8010, Solarbio, Beijing, China) at 37 $^\circ\text{C}$ for 40 min. Cells were reacted with 10 μL of 10 mM 2-DG, followed by glucose consumption measurement. For lactate and ATP determination, 100 μL buffer in the corresponding kits was used to homogenize 1×10^6 cells, and after the mixture was centrifuged, the supernatant was collected, and optical density was determined in the Bio-Rad 680 ELISA reader [24].

Glucose uptake was measured at 590 nm to determine glucose content. The uptake level was calculated based on a standard curve and expressed as relative glucose uptake (%) compared to the controls. Lactate production was tested by

a colorimetric method (570 nm). The lactate concentration in culture supernatant was calculated from a lactate standard curve and presented as relative lactate level (%). ATP levels were detected using a bioluminescence assay based on the luciferin-luciferase reaction. Luminescence was measured with a luminometer. The ATP concentration was measured using an ATP standard curve and was shown as relative ATP content (%).

Flow Cytometry

Detection of cell apoptosis was performed using Annexin V-FITC Apoptosis Detection Kit (C1062L, Beyotime, Shanghai, China). Following digestion, cells were resuspended in 195 μL Annexin V-FITC binding solution and immediately stained with 5 μL Annexin-V-FITC and 10 μL Propidium Iodide (PI) for 20 min in the dark at room temperature. Finally, the apoptosis signal was determined in FACSCantoTM II flow cytometry (BD Biosciences, New Jersey, NY, USA).

qRT-PCR

The extracted total RNA (Trizol Reagent; T9424, Sigma Aldrich, St. Louis, MO, USA) was reverse-transcribed into the first-strand complementary DNA (cDNA) utilizing the Revert Aid cDNA synthesis kit (K1622, Solarbio, Beijing, China). The synthesized cDNA was applied to qRT-PCR by synergy brands Green kit (4385612, ThermoFisher, Waltham, MA, USA) in a real-time PCR instrument (CFX96 Touch, Bio-Rad Laboratories, Inc., Hercules, CA, USA). The reaction was developed at 95 $^\circ\text{C}$ (2 min), followed by 40 cycles (95 $^\circ\text{C}$, 3 sec) and (60 $^\circ\text{C}$, 30 sec). The $2^{-\Delta\Delta\text{CT}}$ method [25] was utilized to process data, and glyceraldehyde-phosphate dehydrogenase (GAPDH) served as the internal control.

Primer sequences included: ROCK1 forward (F), 5'- GAACAAGATAAGGAGCAATC-3', reverse (R), 5'- ACTGGTTCCATCTCTACATC-3'; GAPDH F, 5'-GACAGTCAGCCGCATCTTCT-3', R, 5'-TAAAAGCAGCCCTGGTGAC-3'.

Western Blot Analysis

Proteins extracted from cells (RIPA Buffer; R0010, Solarbio, Beijing, China) were boiled in boiling water (5 min), and underwent concentration measurement using bicinchoninic acid protein assay kit (23227, ThermoFisher, Waltham, MA, USA). Proteins were separated in 6/10% separation gel (P0012AC, Beyotime, Shanghai, China) by sodium dodecyl sulfate-polyacrylamide gel electrophoresis and transferred onto the polyvinylidene fluoride (PVDF) membrane (YA1701, Solarbio, Beijing, China). The membrane was blocked with 5% non-fat milk (D8340, Solarbio, Beijing, China) diluted by Tris Buffered Saline and Tween-20 (T1085, Solarbio, Beijing, China) (1 h, RT), probed with primary antibodies (overnight, 4 $^\circ\text{C}$), and incubated with horseradish peroxidase-conjugated secondary

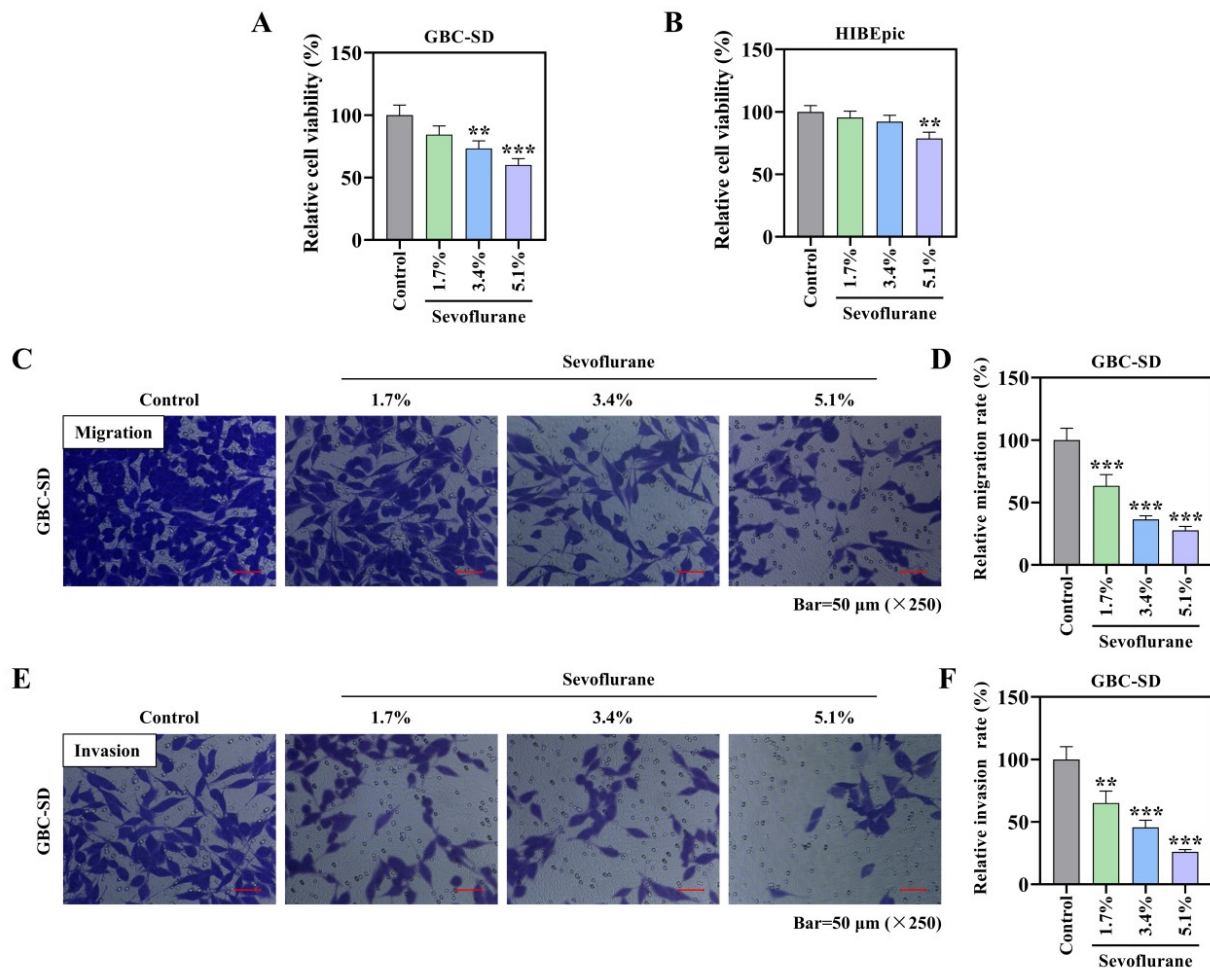


Fig. 1. Sevoflurane suppressed malignancy of GBC cells. (A–F) In HIBEpic and GBC-SD cells exposed to 1.7%, 3.4%, and 5.1% Sevoflurane (6 h) and additionally cultured in a 37 °C incubator (24 h), the viability of two cells (CCK-8 assay) (A,B), as well as the migration and invasion of GBC-SD cells (Transwell assay) ($\times 250$ magnification, scale bar: 50 μm) were conducted (C–F). Data were presented as the mean \pm standard deviation from three independent experiments ($n = 3$). Differences among groups were analyzed by one-way ANOVA, followed by Tukey's post hoc test. *vs. Control, ** $p < 0.01$, *** $p < 0.001$. ANOVA, analysis of variance; GBC, gallbladder cancer; CCK-8, cell counting kit-8.

antibodies (1 h, RT). Following the ECL reagent (FP300, ABP Biosciences, Rockville, Maryland, USA) treatment, band signals analyses were completed on 5200 imaging system (Tanon, Shanghai, China) using ImageJ software (1.52s version, National Institutes of Health, Bethesda, MD, USA), and normalization to GAPDH as a loading control. Data are expressed as fold change relative to the control group.

The related information of antibodies (Abcam, Cambridge, UK) was exhibited below: ROCK1 (ab97592, 158 kDa, 1:1000), ATF4 (ab216839, 38 kDa, 1:1000), CHOP (ab11419, 31 kDa, 1:200), GAPDH (ab8245, 36 kDa, 1:1000); anti-rabbit IgG (ab99697, 1:1000) and anti-mouse IgG (ab6728, 1:2000).

Statistical Analysis

All data analyzed by GraphPad 8.0 (GraphPad Software, San Diego, CA, USA) were presented as the mean \pm standard deviation from three independent experiments ($n = 3$). One-way analysis of variance (ANOVA) followed by Tukey's post hoc test was used for comparison among the multiple groups. The significant variance was indicated at $p < 0.05$.

Results

Sevoflurane Attenuated Malignancy, Activated ER Stress, Inhibited Glycolysis, Downregulated ROCK1 Expression, and Promoted Apoptosis in GBC Cells

Following Sevoflurane treatment with different concentrations, HIBEpic and GBC-SD cells viability was de-

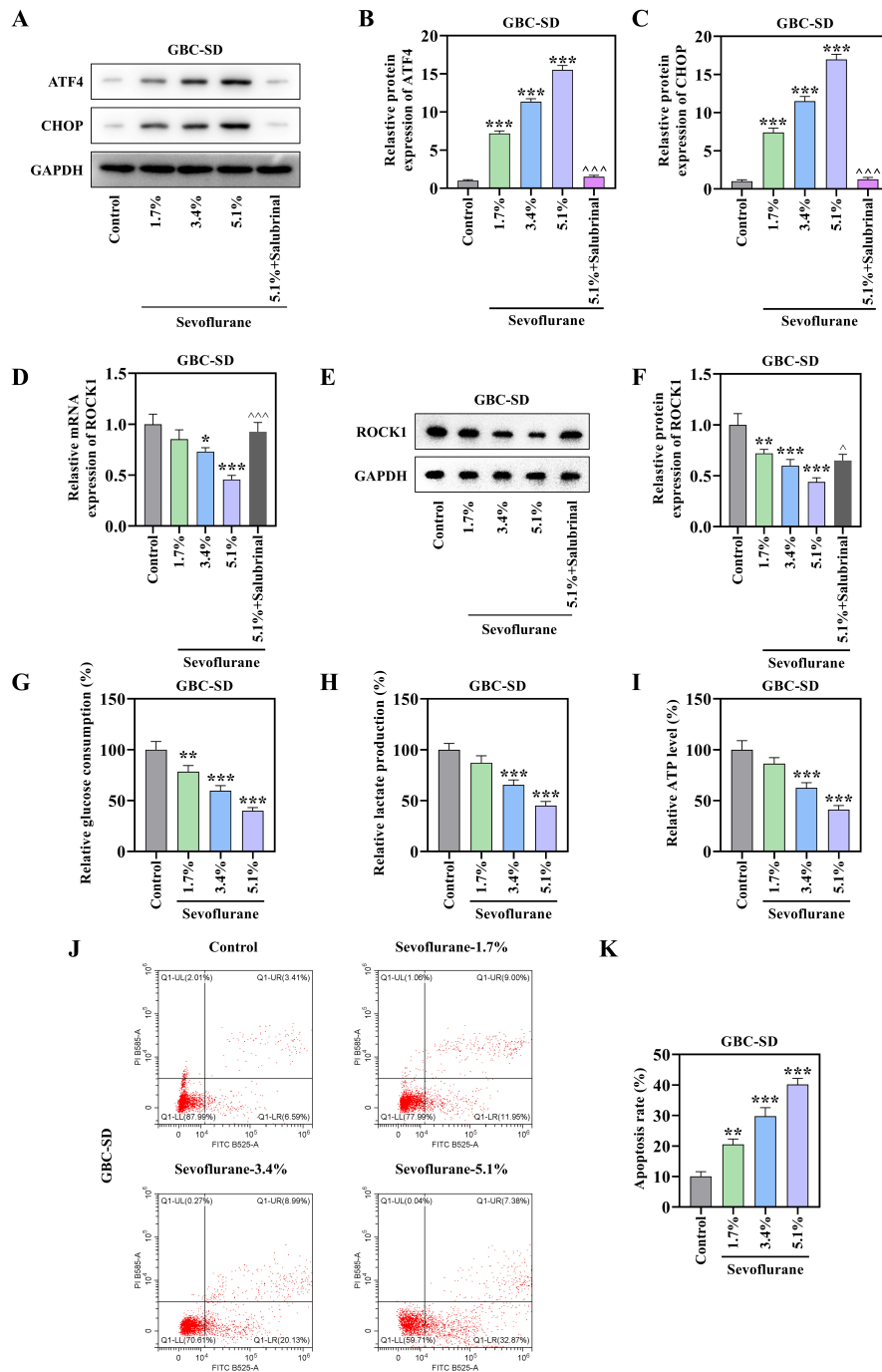


Fig. 2. Sevoflurane activated ER stress, inhibited glycolysis, downregulated ROCK1 expression, and promoted apoptosis of GBC cells. (A–F) ATF4 and CHOP expressions (Western blot analysis) (A–C), ROCK1 mRNA expression (qRT-PCR) and protein expression (Western blot analysis) (D–F) in GBC-SD cells pretreated with 20 μ M Salubrinol (1 h) and exposed in 5.1% Sevoflurane (6 h), with normal GBC-SD cells treated with or without 1.7%, 3.4% and 5.1% Sevoflurane, followed by 24-h incubation in a 37 $^{\circ}$ C incubator (24 h). (G–K) GBC-SD cells exposed to 1.7%, 3.4%, and 5.1% Sevoflurane (6 h) and additionally cultured in a 37 $^{\circ}$ C incubator (24 h). Glucose uptake, lactate and ATP (special kits) (G–I), and apoptosis of GBC-SD cells (flow cytometry) (J,K) were determined. GAPDH served as the loading control in qRT-PCR and Western blot analysis. Data were presented as the mean \pm standard deviation from three independent experiments (n = 3). Differences among groups were analyzed by one-way ANOVA, followed by Tukey's post hoc test. *vs. Control, * p < 0.05, ** p < 0.01, *** p < 0.001. \wedge vs. 5.1%, \wedge p < 0.05, $\wedge\wedge$ p < 0.001. ER, endoplasmic reticulum; ATF4, activating transcription factor 4; CHOP, C/EBP-homologous protein 10; GAPDH, glyceraldehyde-phosphate dehydrogenase; qRT-PCR, quantitative real-time reverse transcription polymerase chain reaction; ROCK1, Rho associated coiled-coil containing protein kinase 1; ATP, adenosine triphosphate.

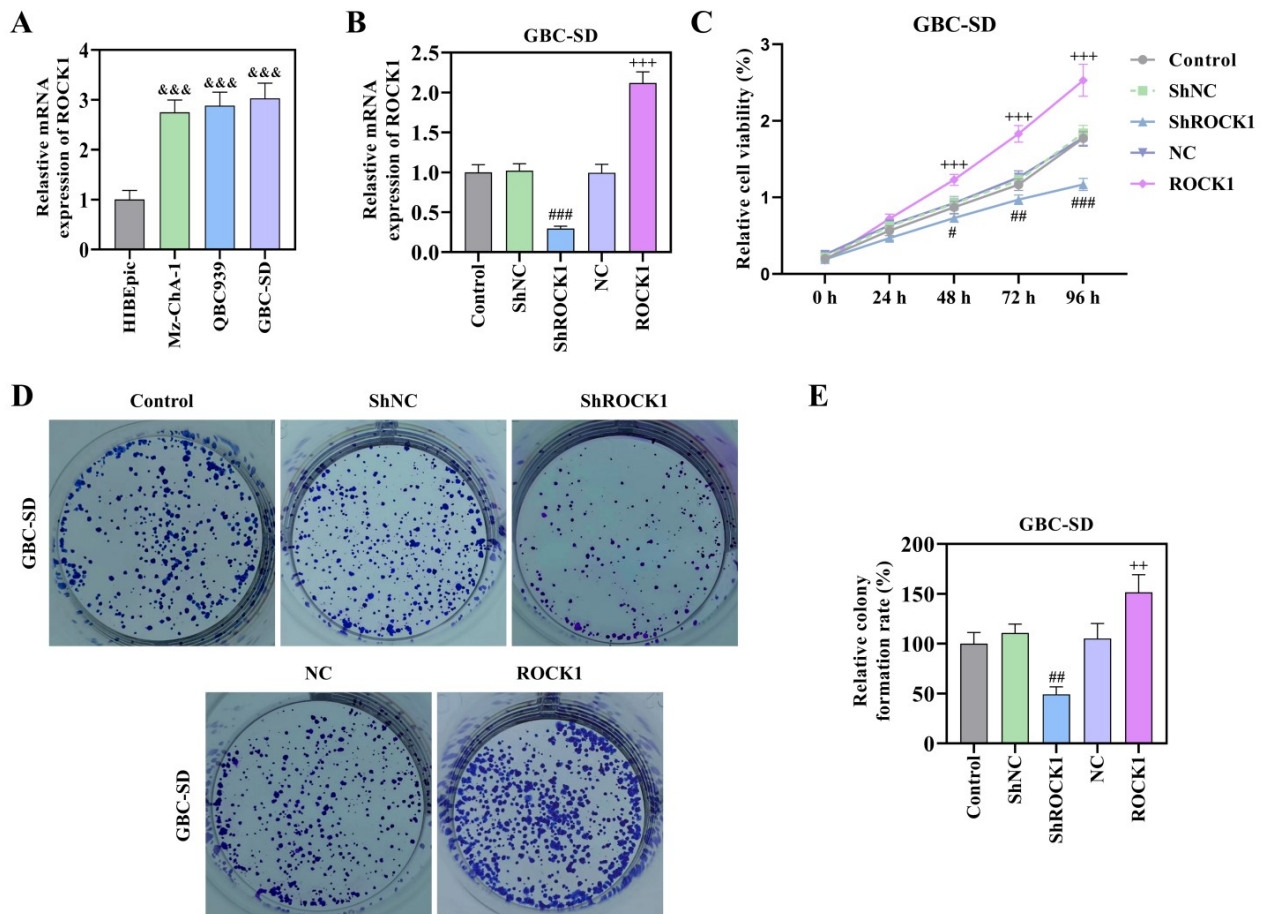


Fig. 3. ROCK1 was highly expressed in GBC cells and promoted the viability and proliferation of GBC cells. (A) ROCK1 expression in normal intestinal biliary epithelial cells HIBEplic and different GBC cell lines Mz-ChA-1, QBC939, and GBC-SD (qRT-PCR). (B–E) GBC-SD cells were transfected with ROCK1-overexpressing vector (ROCK1), NC, ShROCK1, or ShNC; untransfected cells served as controls. Transfection efficiency was evaluated by qRT-PCR (B), cell viability at 0, 24, 48, 72, and 96 h after transfection (CCK-8 assay) (C), and cell proliferation (colony formation assay) (D,E). GAPDH served as the loading control in qRT-PCR. Data were presented as the mean \pm standard deviation from three independent experiments ($n = 3$). Differences among groups were analyzed by one-way ANOVA, followed by Tukey's post hoc test. & vs. HIBEplic, &&& $p < 0.001$. # vs. ShNC, # $p < 0.05$, ## $p < 0.01$, ### $p < 0.001$. + vs. NC, ++ $p < 0.01$, +++ $p < 0.001$. ShROCK1, short hairpin RNA targeting ROCK1; NC, negative control.

terminated. As shown in Fig. 1A,B, 3.4% and 5.1% Sevoflurane significantly inhibited the viability of GBC-SD cells ($p < 0.05$), while only 5.1% Sevoflurane showed the inhibitory effect on the viability of HIBEplic cells ($p < 0.05$), which suggested that GBC cells were more sensitive to Sevoflurane than normal biliary epithelial cells. Subsequently, the measurement of migration (Fig. 1C,D) and invasion (Fig. 1E,F) showed that different concentrations of Sevoflurane suppressed the capability of migration and invasion in GBC-SD cells ($p < 0.05$). These data could demonstrate the suppressive role of Sevoflurane on GBC cell malignancy. To explore the association between Sevoflurane and ER stress, we quantified two ER stress-related proteins, ATF4 and CHOP, in GBC-SD cells treated with Sevoflurane and/or an ER stress inhibitor Salubrinal.

It was exhibited that ATF4 and CHOP expressions were up-regulated in response to different concentrations of Sevoflurane (Fig. 2A–C, $p < 0.05$), while 5.1% Sevoflurane failed to promote their expressions in GBC-SD cells pretreated with Salubrinal (Fig. 2A–C, $p < 0.05$), hinting that Sevoflurane could activate ER stress of GBC cells. In addition, both ROCK1 mRNA and protein expressions were decreased in GBC-SD cells exposed to 3.4% and 5.1% Sevoflurane, while Salubrinal promoted their expression levels in GBC-SD cells treated with 5.1% Sevoflurane (Fig. 2D–F, $p < 0.05$). Glycolysis is an important metabolic mode to energize the rapid proliferation of cancer cells [26]. As shown in Fig. 2G–I, in GBC-SD cells, different concentrations of Sevoflurane decreased the uptake of glucose ($p < 0.05$), and 3.4% and 5.1% Sevoflurane also reduced levels of lactate

and ATP ($p < 0.05$), indicating glycolysis of GBC cells was inhibited by Sevoflurane. Moreover, GBC-SD cell apoptosis was increased under the treatment of different concentrations of Sevoflurane (Fig. 2J,K, $p < 0.05$).

ROCK1 Upregulation Promoted Malignancy and Glycolysis While Inhibiting Apoptosis in GBC Cells

To investigate how ROCK1 influences GBC, its expression in GBC cell lines (Fig. 3A) was determined. The results showed that GBC cell lines (Mz-ChA-1, QBC939, and GBC-SD) had more ROCK1 expression than normal intestinal biliary epithelial cell line HIBEpic ($p < 0.05$). Furthermore, ROCK1-overexpressing vectors and ShROCK1 were used to transfect GBC-SD cells (Fig. 3B, $p < 0.05$), where increased (Fig. 3C, $p < 0.05$) and decreased (Fig. 3C, $p < 0.05$) ROCK1 expression levels were observed at 48 h, 72 h, and 96 h. At the same time, ROCK1 overexpression significantly enhanced the colony formation (Fig. 3D,E, $p < 0.05$), as well as the migration and invasion in GBC-SD cells (Fig. 4A–D, $p < 0.05$), while ROCK1 silencing exerted the opposite effects (Fig. 3D–E, 4A–D, $p < 0.05$). These data demonstrate the promoting effect of ROCK1 on GBC cell malignancy. Besides, ROCK1 also showed a positive impact on glycolysis of GBC-SD cells, as evidenced by the increased levels of glucose uptake, lactate and ATP in ROCK1-overexpressing GBC-SD cells (Fig. 4E–G, $p < 0.05$) and decreased levels of these indices in ROCK1-silencing GBC-SD cells (Fig. 4E–G, $p < 0.05$). Furthermore, ROCK1 overexpression reduced apoptosis in GBC-SD cells (Fig. 4H,I, $p < 0.05$), whereas ROCK1 silencing increased apoptosis (Fig. 4H,I, $p < 0.05$), indicating that ROCK1 inhibits apoptosis in GBC cells.

ROCK1 Overexpression Reversed Effects of Sevoflurane on Viability, Migration, Invasion and Apoptosis in GBC Cells

Following transfection with ROCK1-overexpressing vectors, GBC-SD cells were further treated with 5.1% Sevoflurane, after which the above indices were reassessed. As a result, ROCK1 overexpression reversed Sevoflurane-inhibited ROCK1 expression, viability, migration, and invasion in GBC-SD cells (Fig. 5A–F, $p < 0.05$). Similarly, Sevoflurane-suppressed levels of glucose uptake, lactate and ATP were also offset by ROCK1 overexpression in GBC-SD cells (Fig. 5G–I, $p < 0.05$). Also, Sevoflurane-promoted apoptosis in GBC-SD cells was suppressed by ROCK1 overexpression (Fig. 5J,K, $p < 0.05$). Thus, these results reveal that ROCK1 overexpression attenuated the role of Sevoflurane in viability, migration, invasion and apoptosis in GBC cells.

Discussion

GBC is attributed to a high mortality rate due to its insidious onset and limited treatment options [3], underscor-

ing the urgent need for development of new drugs to improve patient survival. Herein, we confirmed that Sevoflurane held promise in GBS treatment, due to its ability to inhibit the proliferation, migration, and invasion and promote apoptosis in GBC cells. Sevoflurane has been previously found to suppress malignant phenotype of cells in a wide range of cancers [10,12,27], and the same effect was determined in GBC according to our findings. Furthermore, this effect might be mediated by activating ER stress and inhibiting ROCK1-mediated glycolysis.

The impact of Sevoflurane on ER stress remains controversial. While several studies have demonstrated that sevoflurane induces neuronal apoptosis through activation of ER stress [28–30], others have reported that sevoflurane suppresses ER stress and thereby ameliorates cellular injury [31–33]. In the present study, we found that ER stress-related proteins ATF4 and CHOP were upregulated in Sevoflurane-exposed GBC cells. However, pretreatment with an ER stress inhibitor abrogated these effects of Sevoflurane. Our data demonstrated that Sevoflurane could activate ER stress in GBC cells, consistent with previous evidence. Considering that cirsimaritin has been shown to promote apoptosis in GBC cells by inducing ER stress [20], we hypothesize that the inhibitory effects of Sevoflurane on the GBC malignant phenotype mentioned above may depend on activation of ER stress to some degree.

In studies about the antitumor effect of Sevoflurane, ROCK1 has been frequently mentioned. For example, Cheng S and Cheng J [34] indicated that Sevoflurane inhibits ROCK1 expression through circ_0079593/miR-633 axis to suppress glioma tumorigenesis. These findings support the oncogenic role of ROCK1, and suggest that its expression is inhibited in Sevoflurane-exposed cancer cells. Correspondingly, we corroborated the downregulation of ROCK1 mRNA and protein in Sevoflurane-treated GBC cells. However, the role of ROCK1 in GBC remains poorly defined. To investigate the role of ROCK1 in GBC, we determined its expression across different GBC cell lines, revealing high levels of ROCK1. Further, *in vitro* gain- and loss-of-function experiments demonstrated that ROCK1 overexpression promoted proliferation, migration, and invasion, whereas ROCK1 silencing exerted the opposite effects, which clarified that ROCK1 might promote GBC progression.

As is well established, one of the “hallmarks of cancer” is altered energy metabolism, which is defined by a preferential dependence on oxygen-independent glycolysis and increased glucose uptake to adapt to lower ATP production [35]. In a recent study on ovarian cancer, enhanced expression of ROCK1 rescues inhibited glycolysis [36]. In this study, we confirmed the regulation of ROCK1 on glycolysis, and upregulation of glucose uptake, lactate and ATP in ROCK1-overexpressing GBC cells and decreased levels of these indices in ROCK1-silencing GBC cells.

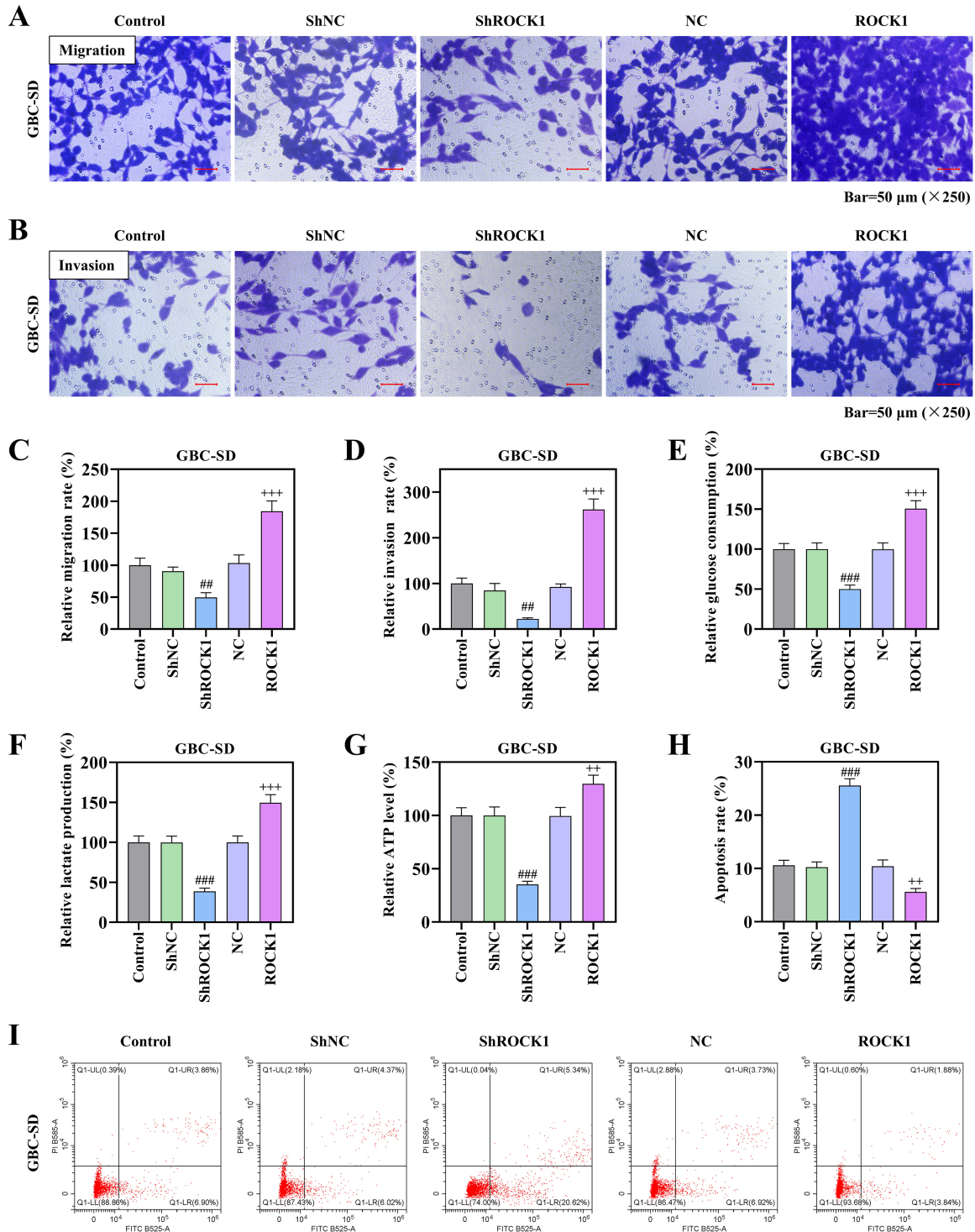


Fig. 4. ROCK1 enhanced migration, invasion, and glycolysis, and inhibited apoptosis in GBC cells. (A–I) Migration and invasion of GBC-SD cells transfected with ROCK1-overexpressing vector (ROCK1), NC, ShROCK1, or ShNC, with untransfected cells as controls (Transwell assay) ($\times 250$ magnification, scale bar: 50 μm) (A–D). Glucose uptake, lactate and ATP (special kits) (E–G), and apoptosis of GBC-SD cells (flow cytometry) (H,I) were determined. Data were presented as the mean \pm standard deviation from three independent experiments ($n = 3$). Differences among groups were analyzed by one-way ANOVA, followed by Tukey's post hoc test. #vs. ShNC, ### $p < 0.01$, #### $p < 0.001$. +vs.NC, ++ $p < 0.01$, +++ $p < 0.001$.

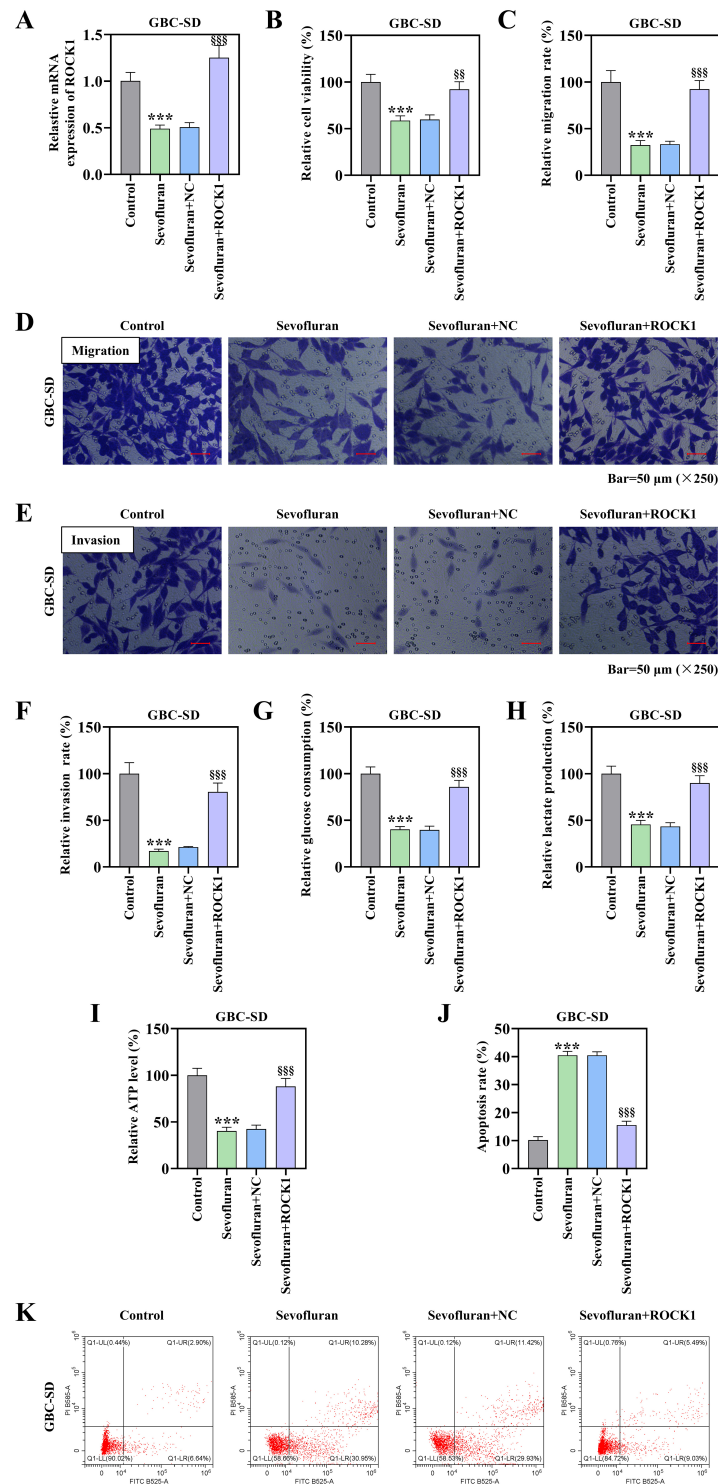


Fig. 5. ROCK1 overexpression reversed effects of Sevoflurane on malignancy, glycolysis and apoptosis in GBC cells. (A–K) GBC-SD cells with or without transfection of ROCK1-overexpressing vectors were exposed to 5.1% Sevoflurane (6 h) and additionally cultured at a 37 °C incubator (24 h). ROCK1 expression (qRT-PCR) (A), cell viability (CCK-8 assay) (B), migration and invasion (Transwell assay) (×250 magnification, scale bar: 50 μm) (C–F), glucose uptake, lactate and ATP (special kits) (G–I), and apoptosis (flow cytometry) (J,K) were detected. GAPDH served as the loading control in qRT-PCR. Data were presented as the mean ± standard deviation from three independent experiments (n = 3). Differences among groups were analyzed by one-way ANOVA. *vs. Control, ***p < 0.001. §vs. Sevofluran+NC, §§p < 0.01, §§§p < 0.001.

Meanwhile, these glycolysis-related indices were also determined in the GBC cells exposed to Sevoflurane, and it was exhibited that Sevoflurane inhibited glycolysis. Considering that ROCK1 was also inhibited by Sevoflurane, we speculated that the suppression of glycolysis by Sevoflurane was mediated by ROCK1. Therefore, we further verified and found that ROCK1 overexpression could attenuate the suppressive impact of Sevoflurane upon the glycolysis of GBC cells. These findings suggest the involvement of ROCK1 in Sevoflurane regulating glycolysis.

This study has several limitations. Firstly, the reliance on *in vitro* experiments using cell lines limits the ability to fully recapitulate the complex tumor microenvironment and systemic effects of Sevoflurane *in vivo*; translating these mechanistic findings into animal models and clinical contexts is therefore essential. Secondly, although ROCK1 is identified as a key mediator, the complete upstream signaling pathways that regulate its downregulation by Sevoflurane remain unclear. Finally, the mechanistic studies were primarily conducted in the GBC-SD cell lines, and future studies across a broader panel of GBC cell lines are needed to validate and generalize our conclusions.

Conclusion

To sum up, this study demonstrates that Sevoflurane may exert antitumor effects in GBC by activating ER stress and suppressing ROCK1-mediated glycolysis. These findings provide a theoretical basis for the potential clinical application of Sevoflurane as a therapeutic agent for GBC.

Availability of Data and Materials

The analyzed data sets generated during the study are available from the corresponding author on reasonable request.

Author Contributions

YL and DZ designed the research study; LZ performed the research; SL and HL collected and analyzed the data. HL has been involved in drafting the manuscript and all authors have been involved in revising it critically for important intellectual content. All authors gave final approval of the version to be published. All authors have participated sufficiently in the work to take public responsibility for appropriate portions of the content and agreed to be accountable for all aspects of the work in ensuring that questions related to its accuracy or integrity.

Ethics Approval and Consent to Participate

Not applicable.

Acknowledgment

Not applicable.

Funding

This research received no external funding.

Conflict of Interest

The authors declare no conflict of interest.

Supplementary Material

Supplementary material associated with this article can be found, in the online version, at <https://doi.org/10.24976/Descov.Med.202638205.33>.

References

- [1] Ganeshan D, Kambadakone A, Nikolaidis P, Subbiah V, Subbiah IM, Devine C. Current update on gallbladder carcinoma. *Abdominal Radiology (New York)*. 2021; 46: 2474–2489. <https://doi.org/10.1007/s00261-020-02871-2>.
- [2] Valle JW, Lamarca A, Goyal L, Barriuso J, Zhu AX. New Horizons for Precision Medicine in Biliary Tract Cancers. *Cancer Discovery*. 2017; 7: 943–962. <https://doi.org/10.1158/2159-8290.CD-17-0245>.
- [3] Rawla P, Sunkara T, Thandra KC, Barsouk A. Epidemiology of gallbladder cancer. *Clinical and Experimental Hepatology*. 2019; 5: 93–102. <https://doi.org/10.5114/ceh.2019.85166>.
- [4] Edgington TL, Muco E, Maani CV. Sevoflurane. *StatPearls*. 2023.
- [5] Zhou X, Liu C, Xia D. Sevoflurane-induced P300 promotes neuron apoptosis via Sp1/CDK9 pathway. *Clinical and Experimental Pharmacology & Physiology*. 2023; 50: 541–553. <https://doi.org/10.1111/1440-1681.13771>.
- [6] Wang Q, Li Y, Tan H, Wang Y. Sevoflurane-Induced Apoptosis in the Mouse Cerebral Cortex Follows Similar Characteristics of Physiological Apoptosis. *Frontiers in Molecular Neuroscience*. 2022; 15: 873658. <https://doi.org/10.3389/fnmol.2022.873658>.
- [7] Zhang Y, Kuai S, Zhang Y, Xue H, Wu Z, Zhao P. Maternal sevoflurane exposure affects neural stem cell differentiation in offspring rats through NRF2 signaling. *Neurotoxicology*. 2022; 93: 348–354. <https://doi.org/10.1016/j.neuro.2022.10.014>.
- [8] Song R, Wang R, Shen Z, Chu H. Sevoflurane diminishes neurogenesis and promotes ferroptosis in embryonic prefrontal cortex via inhibiting nuclear factor-erythroid 2-related factor 2 expression. *Neuroreport*. 2022; 33: 252–258. <https://doi.org/10.1097/WNR.0000000000001775>.
- [9] Zheng F, Wu X, Zhang J, Fu Z. Sevoflurane suppresses NLRP3 inflammasome-mediated pyroptotic cell death to attenuate lipopolysaccharide-induced acute lung injury through inducing GSK-3 β phosphorylation and activation. *International Immunopharmacology*. 2022; 109: 108800. <https://doi.org/10.1016/j.intimp.2022.108800>.
- [10] Quan Y, Li S, Wang Y, Liu G, Lv Z, Wang Z. Propofol and Sevoflurane Alleviate Malignant Biological Behavior and Cisplatin Resistance of Xuanwei Lung Adenocarcinoma by Modulating the Wnt/ β -catenin Pathway and PI3K/AKT Pathway. *Anti-cancer Agents in Medicinal Chemistry*. 2022; 22: 2098–2108. <https://doi.org/10.2174/1871520621666211026092405>.
- [11] Zeng X, Zheng Q, Wang L, Chen T, Lin W, Lin Q. Sevoflu-

- rane suppresses the malignant progression of breast cancer via the hsa_circ_0000129/miR-578/EPSTI1 axis. *Thoracic Cancer*. 2023; 14: 2665–2677. <https://doi.org/10.1111/1759-7714.15053>.
- [12] Ding J, Zhang L, Zeng S, Feng T. Clinically relevant concentration of sevoflurane suppresses cervical cancer growth and migration through targeting multiple oncogenic pathways. *Biochemical and Biophysical Research Communications*. 2019; 514: 1179–1184. <https://doi.org/10.1016/j.bbrc.2019.05.082>.
- [13] Wang X, Chen S, Xiang H, Wang X, Xiao J, Zhao S, *et al.* S1PR2/RhoA/ROCK1 pathway promotes inflammatory bowel disease by inducing intestinal vascular endothelial barrier damage and M1 macrophage polarization. *Biochemical Pharmacology*. 2022; 201: 115077. <https://doi.org/10.1016/j.bcp.2022.115077>.
- [14] Ko E, Kim D, Min DW, Kwon SH, Lee JY. Nrf2 regulates cell motility through RhoA-ROCK1 signalling in non-small-cell lung cancer cells. *Scientific Reports*. 2021; 11: 1247. <https://doi.org/10.1038/s41598-021-81021-0>.
- [15] Ma S, Huang Z, Chen Q, Yin X. Effect of Cichoric Acid on Colorectal Cancer: Impact on Migration, Epithelial-Mesenchymal Transition, and Proliferation via RhoA/ROCK Signaling Pathway Modulation. *Discovery Medicine*. 2024; 36: 190–198. <https://doi.org/10.24976/Discover.Med.202436180.18>.
- [16] Zeng Z, Huang Q, Mao L, Wu J, An S, Chen Z, *et al.* The Pyruvate Dehydrogenase Complex in Sepsis: Metabolic Regulation and Targeted Therapy. *Frontiers in Nutrition*. 2021; 8: 783164. <https://doi.org/10.3389/fnut.2021.783164>.
- [17] Pang S, Shen Y, Wang Y, Chu X, Ma L, Zhou Y. ROCK1 regulates glycolysis in pancreatic cancer via the c-MYC/PFKFB3 pathway. *Biochimica et Biophysica Acta. General Subjects*. 2024; 1868: 130669. <https://doi.org/10.1016/j.bbagen.2024.130669>.
- [18] Ajoolabady A, Kaplowitz N, Lebeauapin C, Kroemer G, Kaufman RJ, Malhi H, *et al.* Endoplasmic reticulum stress in liver diseases. *Hepatology (Baltimore, Md.)*. 2023; 77: 619–639. <https://doi.org/10.1002/hep.32562>.
- [19] Wang L, Liu Y, Zhang X, Ye Y, Xiong X, Zhang S, *et al.* Endoplasmic Reticulum Stress and the Unfolded Protein Response in Cerebral Ischemia/Reperfusion Injury. *Frontiers in Cellular Neuroscience*. 2022; 16: 864426. <https://doi.org/10.3389/fncel.2022.864426>.
- [20] Quan Z, Gu J, Dong P, Lu J, Wu X, Wu W, *et al.* Reactive oxygen species-mediated endoplasmic reticulum stress and mitochondrial dysfunction contribute to cirsimaritin-induced apoptosis in human gallbladder carcinoma GBC-SD cells. *Cancer Letters*. 2010; 295: 252–259. <https://doi.org/10.1016/j.canlet.2010.03.008>.
- [21] Rozpedek W, Pytel D, Mucha B, Leszczynska H, Diehl JA, Majsterek I. The Role of the PERK/eIF2 α /ATF4/CHOP Signaling Pathway in Tumor Progression During Endoplasmic Reticulum Stress. *Current Molecular Medicine*. 2016; 16: 533–544. <https://doi.org/10.2174/1566524016666160523143937>.
- [22] Zheng QY, Li PP, Jin FS, Yao C, Zhang GH, Zang T, *et al.* Ursolic acid induces ER stress response to activate ASK1-JNK signaling and induce apoptosis in human bladder cancer T24 cells. *Cellular Signalling*. 2013; 25: 206–213. <https://doi.org/10.1016/j.cellsig.2012.09.012>.
- [23] Zhu X, Peng C, Peng Z, Chang R, Guo Q. Sevoflurane Inhibits Metastasis in Hepatocellular Carcinoma by Inhibiting MiR-665-Induced Activation of the ERK/MMP Pathway. *Cell Transplantation*. 2022; 31: 9636897221104447. <https://doi.org/10.1177/09636897221104447>.
- [24] Zeng C, Huang D, Wang L, Liang H, Ma X. Silencing ZIC5 suppresses glycolysis and promotes disulfidptosis in lung adenocarcinoma cells. *Cancer Biology & Therapy*. 2025; 26: 2501780. <https://doi.org/10.1080/15384047.2025.2501780>.
- [25] Livak KJ, Schmittgen TD. Analysis of relative gene expression data using real-time quantitative PCR and the 2(-Delta Delta C(T)) Method. *Methods (San Diego, Calif.)*. 2001; 25: 402–408. <https://doi.org/10.1006/meth.2001.1262>.
- [26] Zhang G, Zhao X, Liu W. NEDD4L inhibits glycolysis and proliferation of cancer cells in oral squamous cell carcinoma by inducing ENO1 ubiquitination and degradation. *Cancer Biology & Therapy*. 2022; 23: 243–253. <https://doi.org/10.1080/15384047.2022.2054244>.
- [27] Yan R, Song T, Wang W, Tian J, Ma X. Immunomodulatory roles of propofol and sevoflurane in murine models of breast cancer. *Immunopharmacology and Immunotoxicology*. 2023; 45: 153–159. <https://doi.org/10.1080/08923973.2022.2122501>.
- [28] Zhang Q, Li Y, Wang X, Yin C, Zhou Q, Guo J, *et al.* Sevoflurane exposure causes neuronal apoptosis and cognitive dysfunction by inducing ER stress *via* activation of the inositol 1, 4, 5-trisphosphate receptor. *Frontiers in Aging Neuroscience*. 2022; 14: 990679. <https://doi.org/10.3389/fnagi.2022.990679>.
- [29] Shen FY, Song YC, Guo F, Xu ZD, Li Q, Zhang B, *et al.* Cognitive Impairment and Endoplasmic Reticulum Stress Induced by Repeated Short-Term Sevoflurane Exposure in Early Life of Rats. *Frontiers in Psychiatry*. 2018; 9: 332. <https://doi.org/10.3389/fpsy.2018.00332>.
- [30] Luo D, Chen H, Li X, Lu P, Long M, Peng X, *et al.* Activation of the ROCK1/MMP-9 pathway is associated with the invasion and poor prognosis in papillary thyroid carcinoma. *International Journal of Oncology*. 2017; 51: 1209–1218. <https://doi.org/10.3892/ijo.2017.4100>.
- [31] Lv CM, Wu HM, Wu L, Xu GH, Yang ZL, Shen QY. Sevoflurane modulates AQP5 (1,5) expression and endoplasmic reticulum stress in mice lung with allergic airway inflammation. *BioScience Reports*. 2019; 39: BSR20193282. <https://doi.org/10.1042/BSR20193282>.
- [32] Zhang YQ, Li R, Tian SY, Lv JP, Yang BZ, Wang J, *et al.* Sevoflurane preconditioning protects against acute MI/R injury via enhancing AdipoR1-Cav3 interaction and alleviating endoplasmic reticulum stress. *Experimental Cell Research*. 2022; 417: 113217. <https://doi.org/10.1016/j.yexcr.2022.113217>.
- [33] Wang Y, Ge C, Chen J, Tang K, Liu J. GSK-3 β inhibition confers cardioprotection associated with the restoration of mitochondrial function and suppression of endoplasmic reticulum stress in sevoflurane preconditioned rats following ischemia/reperfusion injury. *Perfusion*. 2018; 33: 679–686. <https://doi.org/10.1177/0267659118787143>.
- [34] Cheng S, Cheng J. Sevoflurane suppresses glioma tumorigenesis via regulating circ_0079593/miR-633/ROCK1 axis. *Brain Research*. 2021; 1767: 147543. <https://doi.org/10.1016/j.brainres.2021.147543>.
- [35] Ganapathy-Kanniappan S, Geschwind JFH. Tumor glycolysis as a target for cancer therapy: progress and prospects. *Molecular Cancer*. 2013; 12: 152. <https://doi.org/10.1186/1476-4598-12-152>.
- [36] Xie W, Liu LU, He C, Zhao M, Ni R, Zhang Z, *et al.* Circ_0002711 knockdown suppresses cell growth and aerobic glycolysis by modulating miR-1244/ROCK1 axis in ovarian cancer. *Journal of Biosciences*. 2021; 46: 21. <https://doi.org/10.1007/s12038-020-00136-0>.